CHAPTER 2

Biosynthesis of poly(ethyleneglycol)-supported palladium nanoparticles using *Colocasia esculanta* (*C. esculanta*) leaf extracts as reducing agent and their catalytic application in Suzuki-Miyaura cross-coupling reaction.

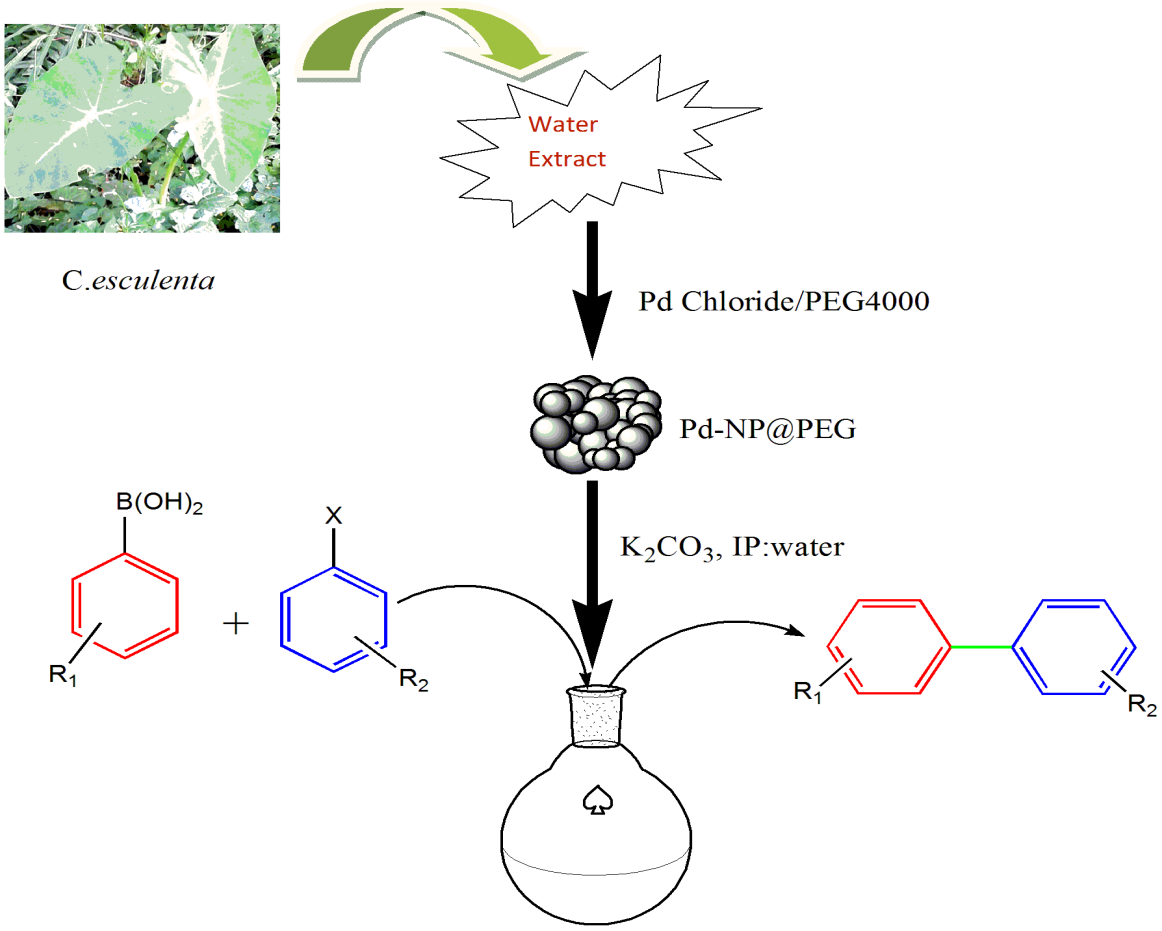

The work described in this chapter has been published in *RSC Advances*, 2015, 5, 72453-72457

2.1 Introduction

The palladium-catalyzed carbon-carbon bond forming reactions developed by Heck, Negishi and Suzuki have made a crucial impact in the scenario of modern synthetic organic chemistry [1, 2]. In this regard, specially, the Suzuki-Miyaura cross-coupling reaction developed in the year 1979 has probably become one of the most widely used methods. Their widespread use is mainly due to the mild nature of organoboron compounds which are generally non-toxic, stable to air, heat and moisture and also with their compatibility to a wide variety of functional groups. Their wide ranges of applications in the production of agrochemicals, polymers, and pharmaceutical intermediates [3, 4] make them more attractive. Again, nowadays, metal NPs because of their high surface area are regarded as very attractive and efficient catalysts in comparison to their bulk counterparts. Also, they behave as heterogeneous catalysts. Pd NPs have gained considerable attention in recent years since they show remarkable physical, chemical, optical and thermodynamical properties [5] and much focused have been given by researchers on their synthesis. Because of these, Pd NPs find wide applications in the field of catalysis [6] and drug delivery [7]. Generally, different wet synthesis processes such as chemical [8], sonochemical [9] and polyols reduction [10] have been used for the synthesis of Pd NPs of different shapes sizes. Though these types of synthesis processes generally provide high growth rate and high yield however, they are not environment friendly and therefore some alternative methods are in continuous search for the synthesis of NPs which are eco-friendly with minimum usages of chemicals. Biological materials such as plant extracts, microorganisms could be used for the synthesis of NPs as they have the reduction potential required for the synthesis and also, they act as stabilizers [11, 12]. As the biosynthesis method do not use any toxic chemical for their synthetic protocols they offer several advantages of eco-friendliness and are compatible for pharmaceutical and other biomedical applications [13]. Also, the processes are cost effective, and can easily be scaled up for large scale synthesis. Compared to microbial synthesis, biosynthesis of NPs using plant extracts is more advantageous as unlike microbial synthesis there is a no need to purify the NPs from microbial contamination. In comparison to other synthetic methods only a few numbers of literature reports are available for the biosynthesis of Pd NPs. Some of the recently

reported biologically synthesis for Pd NPs include peel extract of *Annona squamosa* (sugar-apple) [14], leaf extract of *Anacardium occidentale* (cashew nut) [15], *Cinnamom zeylanicum* (cinnamon) bark extract [16] and *Musa paradisiaca* (banana) peal extracts [17]. In recent years, the biologically synthesized Pd NPs have found various applications in different fields, e.g. in azo dye decolorization [18] and as a catalyst for Heck reaction [19]. Therefore, it is encouraging for researchers to synthesise Pd NPs using different biological materials which can then be used for various environmental and biological applications.

Herein, we report a simple and green protocol for the synthesis of poly(ethylene glycol) (PEG-400) stabilized Pd NPs under ambient condition using aqueous leaf extract of *Colocasia esculanta* (*C. esculanta*) as the bioreducing agent. This is followed by the evaluation of catalytic activity of biosynthesized Pd NPs for efficient Suzuki cross-coupling reaction at room temperature. Locally, *C. esculenta*, is known as "kochu" (Fig. 1) in Assam, a North Eastern State of India and used by native people of Assam in traditional system of medicine. The presence of bio-chemicals such as ascorbic acid, thiamine, riboflavin, niacin, carbohydrates, fats etc. in its leaves are responsible for its reductive potency [20]. Barua and his group have recently reported the synthesis of PEG-400 supported silver NPs using *C. esculenta* leave extract [21]. Different types of spectroscopic and microscopic tools like FT-IR spectroscopy, SEM, TEM techniques etc. are used to characterize the synthesized Pd NPs. The Suzuki cross-coupling reaction between different electronically substituted substrates was also tested with the prepared NPs and good to high yield of the products were found.

2.2 Experimental

2.2.1 General Information

^{1}H and ^{13}C NMR spectra of the synthesized compounds were recorded in a 400 MHz NMR spectrophotometer (JEOL, JNM-ECS) using tetramethylsilane (TMS) as the internal standard. Chemical shifts are expressed in ppm and the coupling constants are expressed in Hertz. Monitoring of the reactions was done by thin-layer-chromatography (TLC) technique using aluminium precoated TLC plates

Fig. 1: Image of *C. esculenta* Linn plant.

with silica gel $60F_{254}$ (Merck). UV light was used to visualize the spots. Products were purified by column chromatography technique using silica gel (60-120 mesh). Büchi B450 melting point apparatus was used for determining the melting points. UV-Visible spectra were analyzed in Shimadzu (UV-2550) UV-Vis spectrophotometer, FT-IR spectra were recorded in a Nicolet (Impact 410) FT-IR spectrophotometer with frequencies expressed in wave numbers (cm^{-1}). The powder XRD pattern was recorded with Rigaku X-ray diffractometer over the range of 2θ =10-80°. It uses Cu K radiation source (0.15419 nm) and has scintillation counter detector. The surface morphology and EDX analysis of the prepared catalyst were done using SEM (JEOL, model JSM-6390 LV operating at an accelerating voltage of 15 kV). Size and distribution of NPs were determined by using JEOL (JEM-2010) TEM equipped with a slow-scan CCD camera at an operating voltage of 200kV. Inductively Coupled Plasma-Optical Emission spectrometry (ICP-OES) study was carried out in Thermo Scientific iCAP 7600.

2.2.2. Materials and chemical reagents

Chemicals were purchased from different commercials firms. Phenylboronic acid was purchased from Alfa-Aesar, potassium carbonate from Qualigens, bromobenzene from G.S. Chemical Testing Labs, Bombay, India and all other chemicals were purchased from Sisco-Research-Laboratories Pvt. Ltd. India. Solvents like hexane and ethyl acetate used for purification purposes were distilled prior to use. The remaining chemicals were used without further purification.

2.2.3 Preparation of the catalyst

First, to prepare the plant extract, 10 gm of the *C. esculenta* leaves was first washed with deionized water to remove dust and then grounded by using a domestic blender. The whole content was then added to 60 mL distilled water in a beaker and then warmed at 50 °C for about 20 minutes with continuous stirring. It was then filtered with the help of a muslin cloth at ambient temperature. The filtrate was treated as aqueous extract and kept for further experiments.

For the preparation of the catalyst Pd NPs@PEG, first 25 mL of 0.001 M $PdCl_2$ was prepared in 5% (w/v) PEG-4000 solution. After that, 5 mL of the aqueous extract (obtained as above) was added to it. During the process, the pH of the solution was kept within 10 and 11 by using 0.1 M NaOH. The solution was then refluxed for one hour at 60 °C. The formation of the NPs was visually monitored by observing the change of colour from light brown to dark brown. The prepared nanocatalyst was separated by centrifugation at 12,000 rpm for 15 minutes. The separated NPs were washed with distilled water (3 times) and then with ethanol in order to make the NPs free from biomaterials and thereafter dried in an oven at 60 °C for two hours.

2.2.4 General experimental procedure for Pd NPs@PEG catalyzed Suzuki reaction

In order to explore the effectiveness of the catalyst in Suzuki-Miyaura reaction, phenylboronic acid and 4-bromonitrobenzene were taken as the model substrates using isopropanol:water (1:1) as the solvent system and K_2CO_3 as a base. No ligand or additive was added during the course of the reaction and also the reactions were performed under aerobic condition and at room temperature (Scheme 1).

In a 50 mL round-bottomed flask, 0.5 mmol of *p*-bromonitrobenzene, 0.55 mmol of phenylboronic acid, 1.5 mmol of potassium carbonate, and 5 wt% of nanocatalyst with respect to boronic acid substrate were added and stirred in isopropanol:water (1:1) solvent system at room temperature for the desired time. The reaction was monitored by using TLC technique. After completion of the reaction, the product was extracted with distilled ethyl acetate (3 times). Then washed with brine (3 times) and dried over Na_2SO_4. Finally, the products were

purified using column chromatography technique (60-120 mesh silica gel, ethyl acetate-hexane solvent mixture).

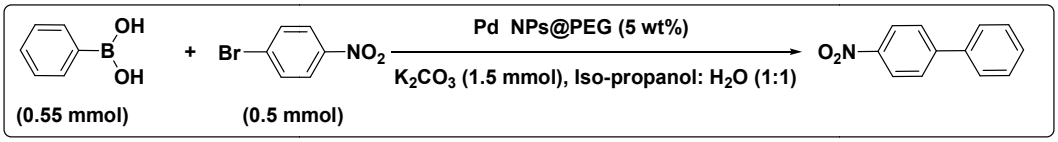

Scheme 1: Optimization of the reaction.

2.3 Results and Discussion

2.3.1 Characterization of the catalyst, Pd NPs@PEG

2.3.1.1 UV-Visible Spectroscopic analysis

The reduction of Pd(II) to Pd(0) using *C. esculenta* leaf extract was first monitored with the help of UV-Vis spectroscopy (Fig. 2). It has been available in a number of reports that basic condition is essential for the synthesis of NPs using plant extract. Keeping this in mind, we adjusted the pH of the reaction solution within 10 and 11 by using 0.1 M NaOH.

During visual monitoring of the reaction, we observed a gradual shifting of the colour of the solution from light brown to dark brown within 1 hr at moderate temperature. Due to excitation of Surface Plasmon Resonance (SPR) of Pd NPs formed, the change of colour from light brown to dark brown was observed. Due

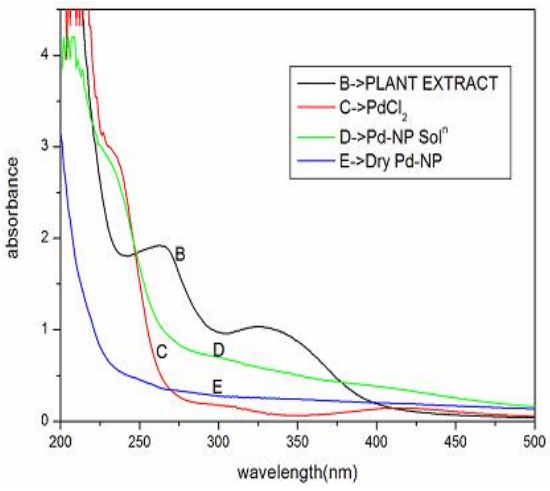

Fig. 2: UV-Visible spectra of B) plant extract, C) $PdCl_2$ solution, D) Pd NPs solution after bio reduction and E) dry Pd NPs.

to the presence of Pd(II) ion in the solution, a distinct peak near 300 nm was observed for $PdCl_2$ solution in the UV-Vis spectroscopy. However, as time proceeds, the peak near 300 nm begins to disappear and vanishes within 2 h which may be due to the transfer of metal charge from Pd(II) to Pd(0). The appearance of a broad continuous spectrum, with gradual increase in intensity from visible to UV region confirms the complete reduction of Pd(II) to Pd(0).

2.3.1.2 FT-IR spectroscopic analysis

The typical FT-IR spectra for the plant extract and biosynthesized Pd NPs are shown in the figure below (Fig. 3). The aqueous extract of *C. esculenta* leaf shows the presence of biomolecules like ascorbic acid (vitamin C), thiamine, riboflavin, niacin, carbohydrates (glucose, fructose, sucrose etc), fats etc [20]. These biomolecules possess number of hydroxyl groups which are mainly responsible for the reduction of the divalent palladium and in turn transform into corresponding carbonyl groups. The FT-IR spectrum of the plant extract shows a peak at 3438 cm^{-1} which is due to the surface hydroxyl groups. The other notable peak at 1622 cm^{-1} is due to C=O stretching vibration of ascorbic acid present in the leaf extract. The peak for hydroxyl group at 3438 cm^{-1} shown in the IR spectrum of plant extract indicates that the surface hydroxyl groups available in the bioactive molecules mainly reduces Pd(II) and correspondingly transformed into carbonyl groups. The presence of peaks at 3395 cm^{-1}, 1622 cm^{-1} and 1073 cm^{-1} clearly indicate that different polyol compounds are adsorbed on the palladium surface which are responsible for capping and stabilization of Pd NPs.

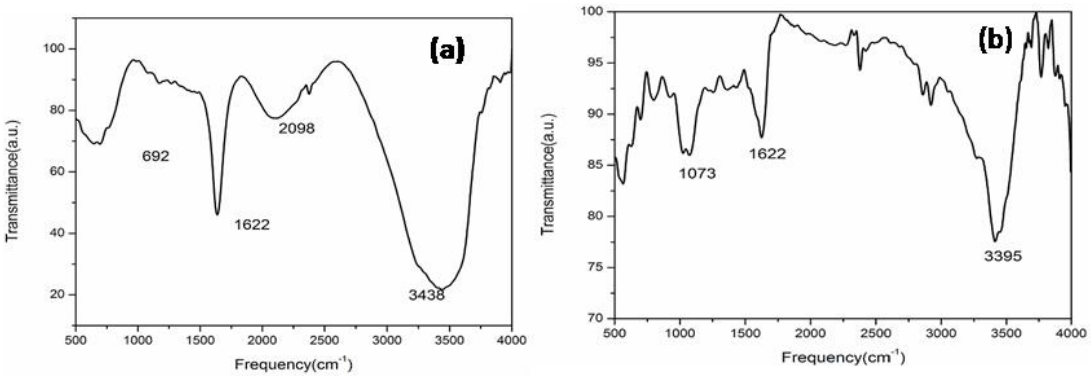

Fig. 3: FT-IR spectra of (a) the plant extract and (b) biosynthesized Pd NPs.

2.3.1.3 Powder XRD analysis

This technique was used to determine the crystal domain size and the structure of the NPs formed. The XRD pattern for both $PdCl_2$ and Pd NPs are plotted in Fig. 4 below. The presence of three peaks at 40.260°, 45.780° and 68.670° corresponding to reflections from (111), (200) and (220) planes respectively that could be indexed to fcc phase of Pd NPs (JCPDS≠89-4897). The broadening of the XRD peak reveals that the synthesized particles are in the nano range.

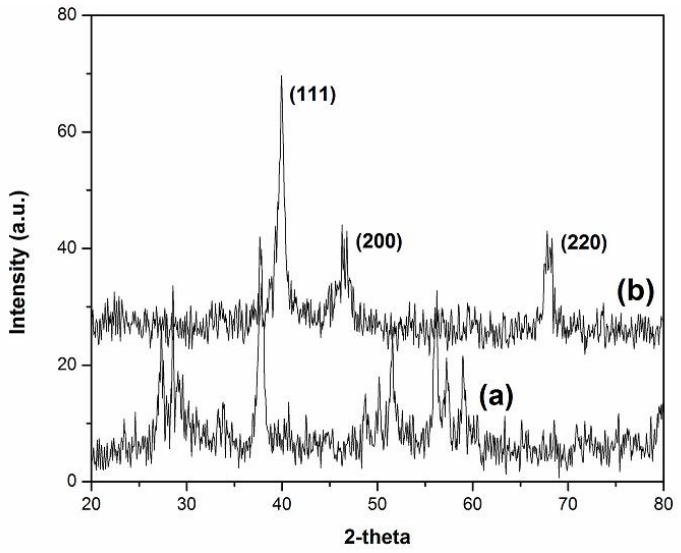

Fig.4: PXRD pattern of (a) $PdCl_2$ and (b) Pd NPs

2.3.1.4 SEM and EDX analyses

SEM analysis was done to determine the surface morphology of the particles and is shown in Figure 5 below**.** The SEM analysis reveals that the prepared NPs have irregular shapes and sizes which may be due to agglomerization of the particles.

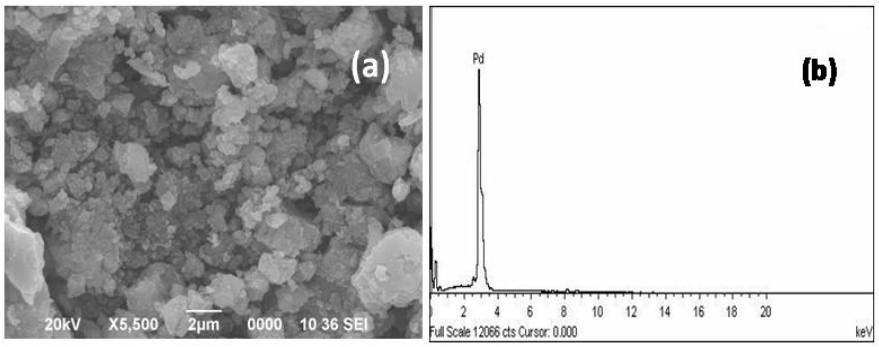

Fig. 5: (a) SEM image and (b) EDX spectrum of Pd NPs

EDX analysis clearly reveals the presence of Pd NPs devoid of any other impurities (Fig. 5).

2.3.1.5 TEM analysis

The synthesized Pd NPs are characterized using TEM and HRTEM measurements for determining the size and shape (Fig. 6). From TEM image, we can say that the NPs mostly crystallize in spherical shape. The inter planer distance of 0.194 nm as calculated from the HRTEM image [Fig. 6(b)] corresponds to (200) plane of Pd NPs. From the size distribution plot [Fig. 6(c)] we found that most of the particles fall in the range 4-7 nm size with an average particle diameter of about 5.5 nm.

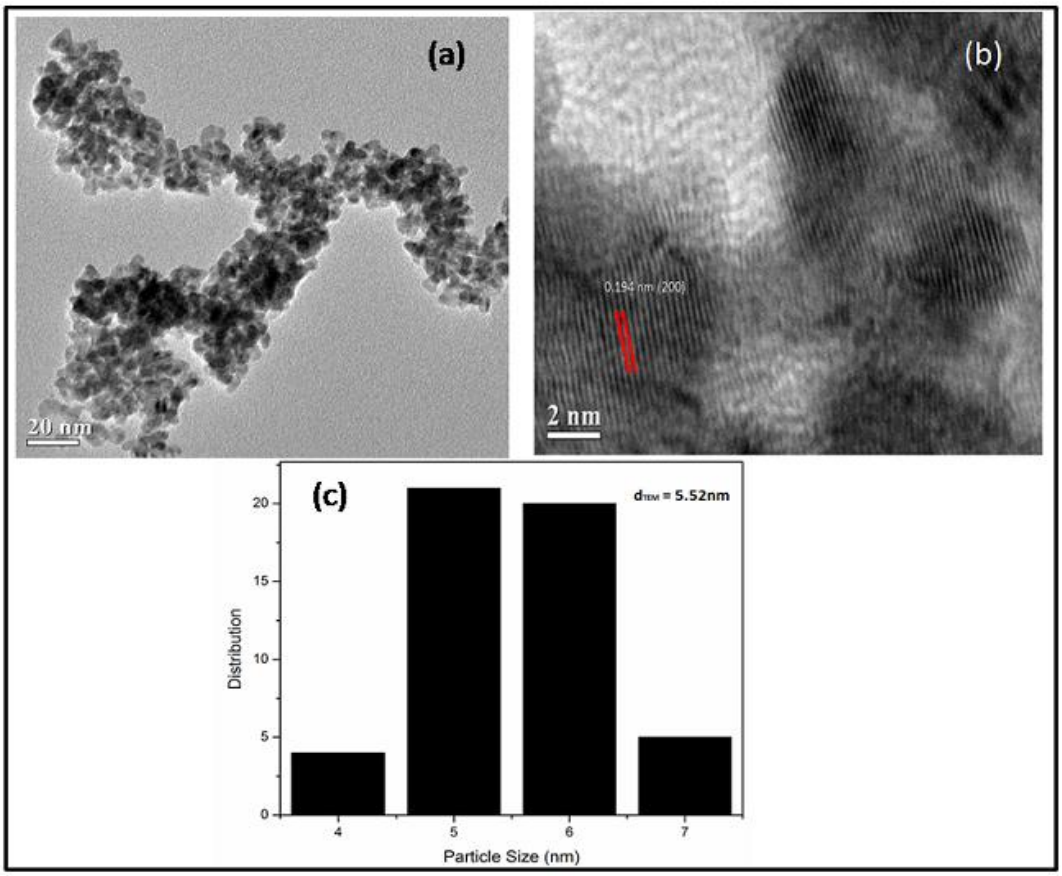

Fig. 6: (a) and (b) TEM image and HRTEM image and (c) particle size distribution of Pd NPs.

2.3.2 Optimization of the reaction condition with respect to solvent, base and catalyst

To investigate the effect of different solvents and bases on the reaction, we have chosen 4-bromonitrobenzene and phenylboronic acid as our model substrates. The results are summarized in Table 1. On screening the effect of solvents using K_2CO_3 as base we found that isopropanol:water (1:1) was the most effective solvent system with excellent yield (entry 7, Table 1). It was also evident from our study that presence of base was crucial for the coupling reaction, since the reaction did not proceed in the absence of a base (entry 2, Table 1). Apart from K_2CO_3, other inorganic bases like Na_2CO_3, KOH are also effective for the cross-coupling reaction with comparable yields (entries 8 and 9, Table 1). However, by considering the cost, efficiency and reliability factors, K_2CO_3 was chosen as the optimized base.

Table 1: Optimization of the reaction condition for base and solvent[a]

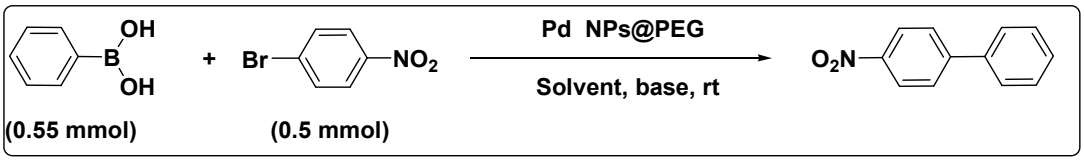

Entry	Solvent	Base	Time (h)	Yield[b]
1	No solvent	K_2CO_3	5	15
2	H_2O	No base	24	No reaction
3	H_2O	K_2CO_3	24	23
4	DMF	K_2CO_3	24	70
5	MeOH:MeCN (1:1)	K_2CO_3	26	45
6	MeOH:H_2O (1:1)	K_2C0_3	28	36
7	Isopropanol:H_20 (1:1)	K_2CO_3	1.5	94
8	Isopropanol:H_20 (1:1)	Na_2CO_3	2.5	90
9	Isopropanol:H_20 (1:1)	KOH	3	85

[a]Reaction Condition: 0.5 mmol 4-bromonitrobenzene, 0.55 mmol phenyl boronic acid, 1.5 mmol base, 3 wt% catalyst and 4 mL solvent.
[b]Isolated yield.

After optimizing the reaction for the solvent system and base, we studied the effect of amount of catalyst on the reaction rate and found that 5 wt% of the catalyst was the optimized amount for the coupling reaction. The results are summarized below (Table 2).

Table 2: Optimization of the reaction condition for the amount of catalyst

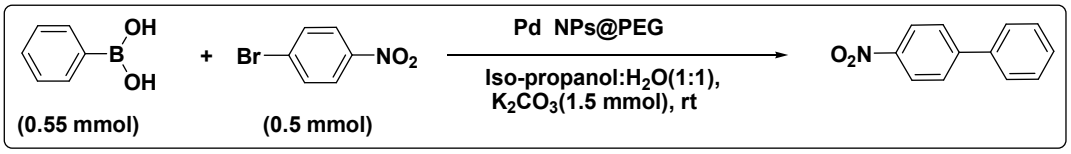

Entry	Catalyst's amount[a] (wt/%)	Time (h)	Yield[b]
1	3	1.5	90
2	5	1.5	94
3	6.5	1.3	94
4	10	1	94

[a]wt % w.r.t. the phenyl boronic acid derivative.
[b]Isolated yield.

2.3.3 Substrate study

With the optimized reaction condition in hand, we next evaluate the scope and limitation of the current reaction procedure, by using a wide range of electronically diverse aryl bromides and iodides with different phenylboronic acid substrates. The results are summarized in table 3.

It was obvious from the substrate study that the cross-coupling reaction between different electron donating and electron withdrawing groups present on the aryl halide and the arylboronic acids proceeded smoothly catalysed by the synthesized Pd NPs. However, if the arylboronic acid contains electron donating group then the reaction requires less time for completion in comparison to electron withdrawing substituent. The monitoring of the reaction was done by TLC technique and the products were characterized using ^{1}H NMR and ^{13}C NMR spectroscopy and melting point determination.

Table 3: Suzuki-Miyaura cross-coupling reaction of various aryl halides with arylboronic acids using Pd NPs@PEG as catalyst[a]

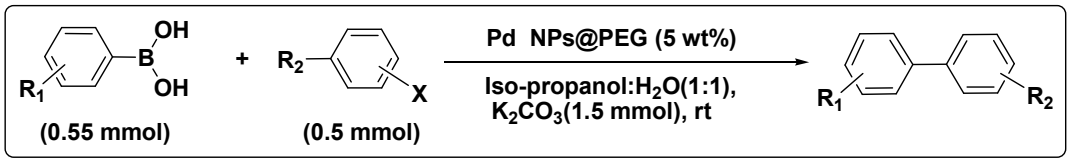

Entry	R_1	X	R_2	Time (h)	Yield[b]
1	H	4-Br	H	1.5	92
2	H	4-Br	NO_2	1.5	94
3	H	4-I	MeO	2	95
4	2-MeO	4-Br	H	1.5	95
5	4-MeO	4-I	MeO	1	92
6	2-Me	4-I	MeO	1	92
7	3-Me	4-Br	MeO	2	91
8	4-CHO	4-Br	H	2	90
9	4-CHO	4-I	MeO	1.5	90
10	4-*tert*-Butyl	4-Br	NO_2	1.5	83
11	2-CHO	4-Br	H	1.5	96
12	2-NH_2	4-Br	H	2	94
13	H	4-Cl	NO_2	24	15

[a]Reaction Conditions: 0.5 mmol halobenzene, 0.55 mmol phenylboronic acid, 1.5 mmol K_2CO_3, 5 wt% catalyst and 4 mL solvent.

[b]Isolated yield

2.3.4. Catalyst reusability study

From the green chemistry point of view, the reusability of catalyst is one of the most important attributes; therefore, we also investigated the reusability of our prepared catalyst. For investigating the reusability of the catalyst, a reaction between 1.65 mmol phenylboronic acid and 1.5 mmol 4-bromonitrobenzene taking as model substrates, 4.5 mmol K_2CO_3 as base, 5 wt% catalyst in 10 mL iso-propanol:H_2O (1:1) was carried out at room temperature. For recovery issue, the scale of the model reaction was increased three times.

It is obvious from the Figure 7 that the catalyst is reusable up to third cycles without any significant loss of the catalytic activity. After third cycle, the catalytic

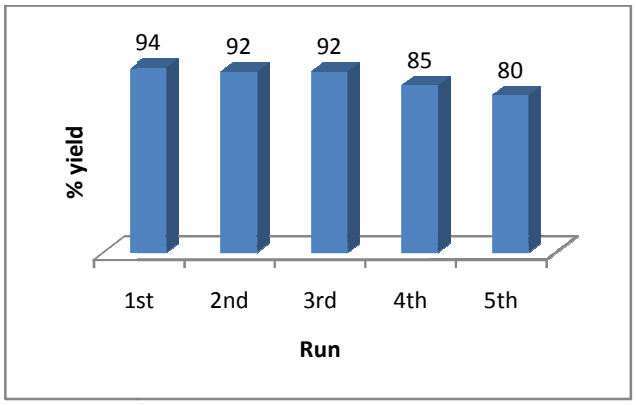

Fig. 7: Reusability of the catalyst.

activity decreases which may be due to the deactivation of the catalyst during the course of the reaction and recovery process. The soluble metal content in the solution was also studied using ICP-OES analysis and we observe only a trace amount of Pd species leaches from the catalyst during the Suzuki-Miyaura cross-coupling reaction. Although a trace amount of Pd leaching was observed, which have no effect on the reaction after filtering off the catalyst, showed that the leached Pd species did not catalyze the Suzuki-Miyaura cross-coupling reaction.

2.3.5. Hot filtration study

The heterogeneous nature of the catalyst was done by hot filtration study (Fig. 8). To do this the model reaction was again performed under the optimized reaction conditions. After 50 min the reaction was stopped and approximately 56% isolated

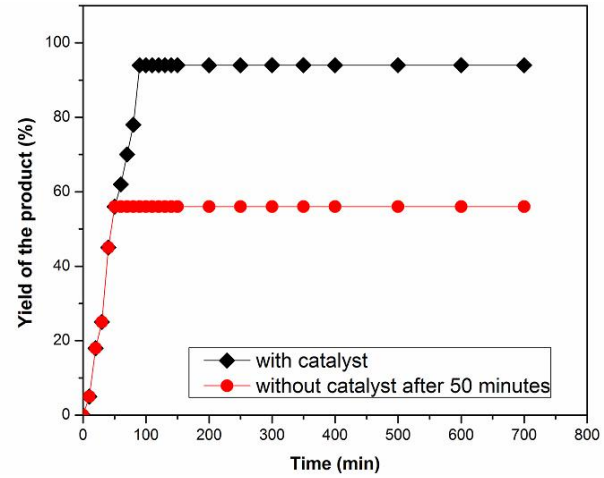

Fig. 8: Hot filtration test.

product yield was recorded. The catalyst was then removed through filtration and the filtrate was allowed to proceed for another 12 h, but we didn't observe any significant increase in the yield of the cross-coupling product, which proves the heterogeneity of the catalyst.

2.4. Conclusions

In conclusion, a green and efficient process for the synthesis of Pd NPs using *C. esculenta* plant extract has been developed which exhibit excellent catalytic activity under mild conditions for Suzuki-Miyaura cross-coupling reaction at room temperature. The polyol and the heterocyclic compounds found in the *C. esculenta* leaves are found to be responsible for the reduction of process and thereby eliminate the use of toxic reducing agents. Therefore, we can consider the synthetic process as green synthesis. Furthermore, the catalyst was found to be recyclable upto 3rd run with slight decrease of the catalytic activity and product yield. The decrease may be due to the deactivation of the catalyst during the course of the reaction and recovery process.

Characterization data of the product

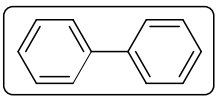

Biphenyl (entry 1, Table 3): White crystal, m.p. 69.2 °C, ^{1}H NMR (400 MHz, $CDCl_3$) δ (ppm): 7.60 (m, 4H), 7.45 (m, 4H), 7.41 (m, 2H); ^{13}C NMR (100 MHz, $CDCl_3$) δ (ppm): 141.3, 128.8, 127.3, 127.2.

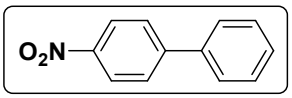

4-Nitrobiphenyl (entries 2 & 13, Table 3): Colorless crystal, m.p. 113 °C, ^{1}H NMR (400 MHz, $CDCl_3$)δ (ppm): 8.30 (m, 2H), 7.75-7.72 (m, 2H), 7.62 (d, J = 8 Hz, 2H), 7.60-7.50 (m, 3H); ^{13}C NMR (100 MHz, $CDCl_3$) δ (ppm): 147.7, 147.1, 138.8, 129.2, 129.0, 127.8, 127.4, 124.1.

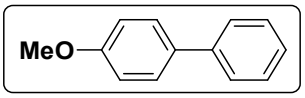

4-Methoxybiphenyl (entry 3, Table 3): White crystal, m.p. 89 °C, ^{1}H NMR (400 MHz, $CDCl_3$)δ (ppm): 7.54 (t, *J* = 8 Hz, 4H), 7.43-7.41 (m, 2H), 7.30-7.25 (m, 1H), 6.99-6.96 (m, 2H), 3.83 (s, 3H); ^{13}C NMR (100 MHz, $CDCl_3$) δ (ppm): 159.2, 140.9, 133.8, 128.8, 128.2, 126.8, 126.7, 114.2, 55.4.

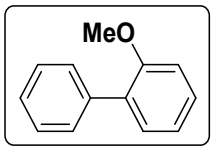

2-Methoxybiphenyl (entry 4, Table 3): Yellow oily liquid, m.p. 30 °C, ^{1}H NMR (400 MHz, $CDCl_3$)δ (ppm): 7.42 (d, *J* = 8 Hz, 2H), 7.30-7.28 (m, 2H), 7.20-7.19 (m, 3H), 6.90-6.87 (m, 1H), 6.84 (d, *J* = 8 Hz, 1H), 3.6 (s, 3H); ^{13}C NMR (100 MHz, $CDCl_3$) δ (ppm): 156.6, 138.7, 131.1, 130.9, 129.7, 128.8, 128.2, 126.9, 121.0, 111.4, 55.7.

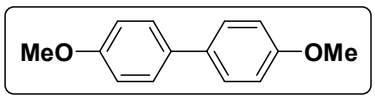

4, 4′-dimethoxybiphenyl (entry 5, Table 3): White Crystalline solid, m.p. 175.5 °C, ^{1}H NMR (400 MHz, $CDCl_3$) δ (ppm): 7.47 (d, *J* = 8 Hz, 4H), 6.95 (d, *J* = 8 Hz, 4H), 3.83 (s, 6H); ^{13}C NMR (100 MHz, $CDCl_3$) δ (ppm): 158.7, 133.5, 127.8, 114.2, 55.4.

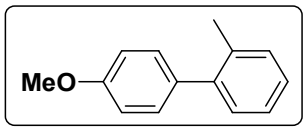

2-Methyl-4'-methoxybiphenyl (entry 6, Table 3): Colourless oil, ^{1}H NMR (400 MHz, $CDCl_3$) δ (ppm): 7.53-7.50 (m, 2H), 7.36-7.25 (m, 3H), 7.15-7.10 (m, 1H), 6.98-6.95 (m, 2H), 3.84 (s, 3H), 2.40 (s, 3H); ^{13}C NMR (100 MHz, $CDCl_3$) δ (ppm): 159.1, 140.8, 138.3, 133.3, 128.7, 128.2, 127.6, 127.4, 123.9, 114.2, 55.4, 21.6.

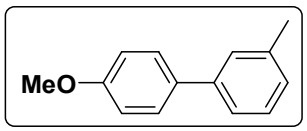

3-Methyl-4'-methoxybiphenyl (entry 7, Table 3): White Crystalline solid, m.p. 51 °C, ^{1}H NMR (400 MHz, $CDCl_3$) δ (ppm): 7.52-7.49 (m, 2H), 7.35-7.29 (m, 3H), 7.15-7.10 (m, 1H), 6.97-6.94 (m, 2H), 3.83 (s, 1H), 2.40 (s, 3H); ^{13}C NMR (100 MHz, $CDCl_3$) δ (ppm): 159.1, 140.9, 138.3, 133.9, 128.7, 128.2, 127.6, 127.5, 123.9, 114.2, 55.4, 21.6.

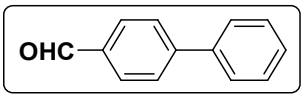

4-Formylbiphenyl (entry 8, Table 3): White crystal, m.p. 58 °C, ^{1}H NMR (400 MHz, $CDCl_3$) δ (ppm): 10.06 (s, 1H), 7.95 (d, *J* = 8 Hz, 2H), 7.71 (d, *J* = 8 Hz, 3H), 7.56 (d, *J* = 8 Hz, 2H), 7.45 (d, *J* = 8 Hz, 2H); ^{13}C NMR (100 MHz, $CDCl_3$) δ (ppm): 191.4, 145.9, 138.2, 135.4, 134.8, 130.4, 129.3, 128.6, 127.6.

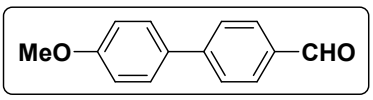

4-Formyl-4'-methoxybiphenyl (entry 9, Table 3): White crystal, m.p. 98 °C, ^{1}H NMR (400 MHz, $CDCl_3$) δ (ppm): 10.03 (s, 1H), 7.93 (d, *J* = 8 Hz, 2H), 7.72 (d, *J* = 8 Hz, 2H), 7.61-7.58 (m, 2H), 7.01 (d, *J* = 8 Hz, 2H), 3.87 (s, 3H); ^{13}C NMR (100 MHz, $CDCl_3$) δ (ppm): 191.9, 159.2, 134.7, 130.4, 128.5, 127.1, 114.5, 55.4.

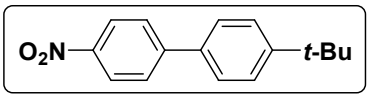

4-Nitro-4'-*tert*-butylbiphenyl (entry 10, Table 3): White crystal, m.p. 160 °C, ^{1}H NMR (400 MHz, $CDCl_3$) δ (ppm): 8.28 (d, *J* = 8 Hz, 2H), 7.73 (d, *J* = 8 Hz, 2H), 7.59-7.51 (m, 4H), 1.37 (s, 9H); ^{13}C NMR (100 MHz, $CDCl_3$) δ (ppm): 152.3, 147.5, 146.9, 135.8, 127.6, 127.1, 126.2, 124.1, 34.8, 31.3.

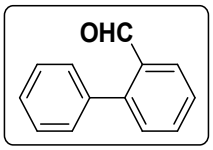

2-Formylbiphenyl (entry 11, Table 3): Brown liquid, ^{1}H NMR (400 MHz, $CDCl_3$) δ (ppm): 9.98 (s, 1H), 8.0 (m, 1H), 7.66-7.63 (m, 1H), 7.50-7.44 (m, 5H), 7.40-7.37 (m, 2H); ^{13}C NMR (100 MHz, $CDCl_3$) δ (ppm): 192.6, 146.0, 137.8, 133.7, 133.6, 130.8, 130.4, 128.5, 128.2, 127.8, 127.6.

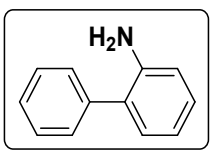

2-Aminobiphenyl (entry 12, Table 3): White crystal, m.p. 51.6 °C, ^{1}H NMR (400 MHz, $CDCl_3$) δ (ppm): 7.57-7.55 (m, 2H), 7.43-7.39 (m, 2H), 7.38-7.25 (m, 1H), 7.24-7.22 (m, 1H), 7.21-6.95 (m, 1H), 6.91-6.90 (m, 1H), 6.73-6.71 (m, 1H), 3.73 (s, br, 2H); ^{13}C NMR (100 MHz, $CDCl_3$) δ (ppm): 146.7, 142.5, 141.4, 129.7, 128.7, 127.3, 127.2, 117.7, 114.1, 113.9

^{1}H Spectrum of 4-nitrobiphenyl

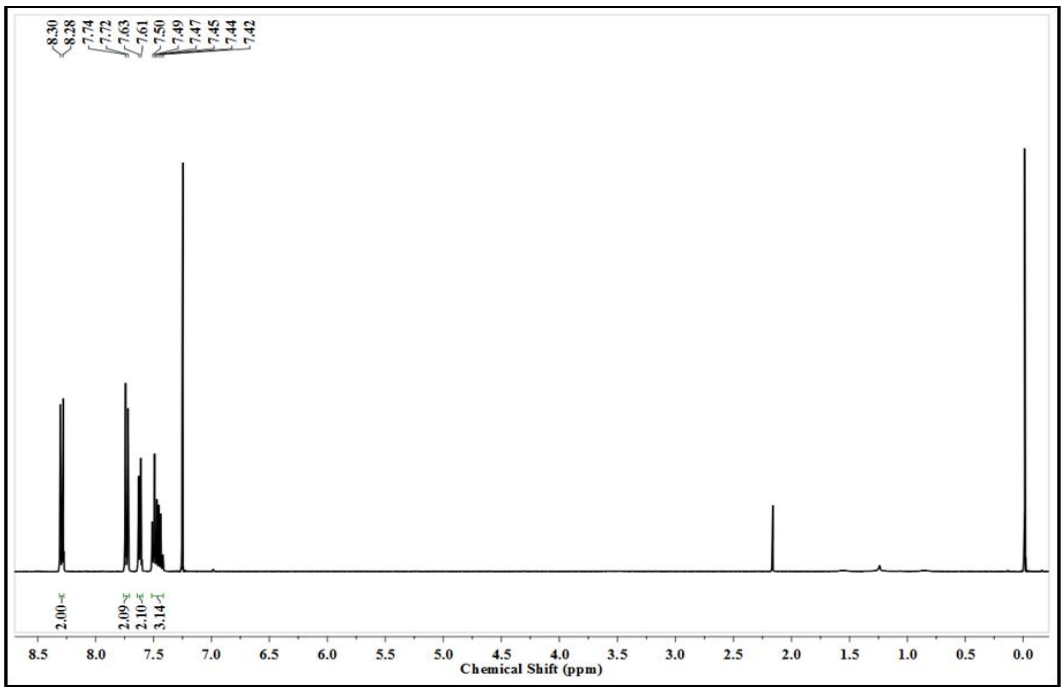

^{13}C NMR spectrum of 4-nitrobiphenyl

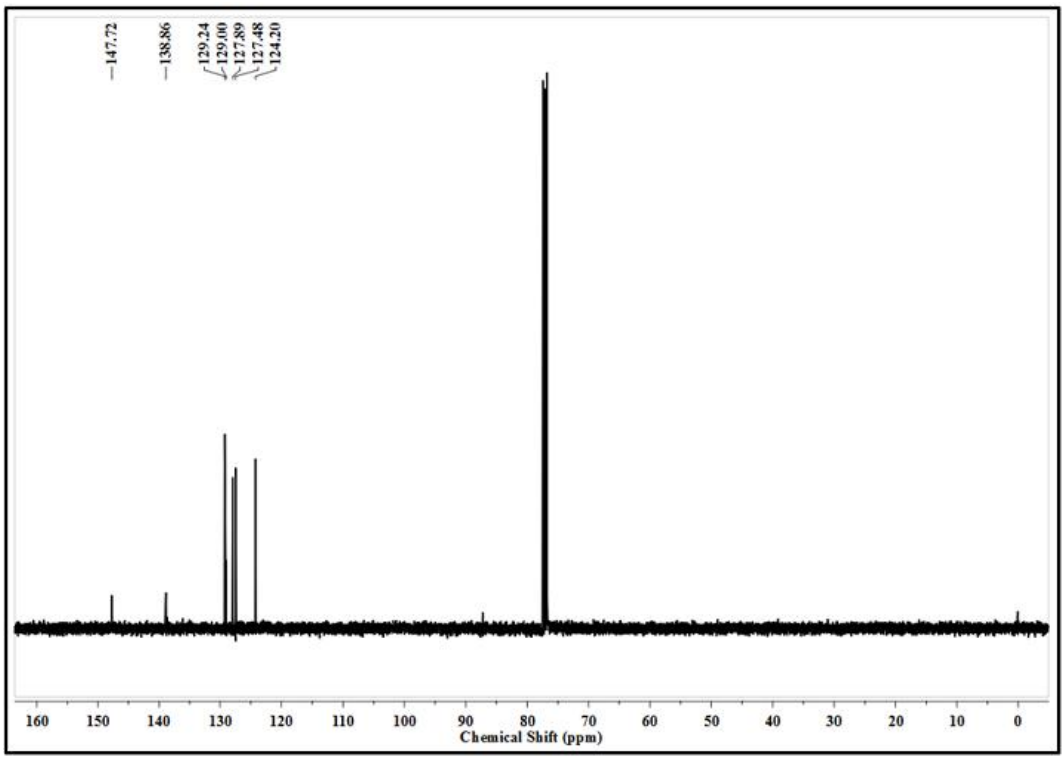

References

[1] Anastasia, L. and Negishi, E. I. Palladium-catalyzed aryl–aryl coupling. In Negishi, E. I. editor, *Handbook of Organopalladium Chemistry for Organic Synthesis*, pages 311-334, Wiley, 2002.

[2] Diederich, F. and Stang, P. J. *Metal-catalyzed cross-coupling reactions*. John Wiley & Sons, 2008.

[3] Torborg, C. and Beller, M. Recent applications of palladium-catalyzed coupling reactions in the pharmaceutical, agrochemical, and fine chemical industries. *Advanced Synthesis & Catalysis*, 351(18):3027-3043, 2009.

[4] Magano, J. and Dunetz, J. R. Large-scale applications of transition metal-catalyzed couplings for the synthesis of pharmaceuticals. *Chemical Reviews*, 111(3):2177-2250, 2011.

[5] Chou, K. S., Lu, Y. C., and Lee, H. H. Effect of alkaline ion on the mechanism and kinetics of chemical reduction of silver. *Materials Chemistry and Physics*, 94(2-3):429-433, 2005.

[6] Chen, R., Jiang, Y., Xing, W., and Jin, W. Preparation of palladium nanoparticles deposited on a silanized hollow fiber ceramic membrane support and their catalytic properties. *Industrial & Engineering Chemistry Research*, 52(14):5002-5008, 2013.

[7] Ghosh, P., Han, G., De, M., Kim, C. K., and Rotello, V. M. Palladium nanoparticles in delivery applications. *Adv. Drug Delivery Rev.*, 60:1307-1315, 2010.

[8] Flanagan, K. A., Sullivan, J. A., and Müeller-Bunz, H. Preparation and characterization of 4-dimethylaminopyridine-stabilized palladium nanoparticles. *Langmuir*, 23(25):12508-12520, 2007.

[9] Nemamcha, A., Rehspringer, J. L., and Khatmi, D. Synthesis of palladium nanoparticles by sonochemical reduction of palladium (II) nitrate in aqueous solution. *The Journal of Physical Chemistry B*, 110(1):383-387, 2006.

[10] Xiong, Y., Chen, J., Wiley, B., Xia, Y., Aloni, S., and Yin, Y. Understanding the role of oxidative etching in the polyol synthesis of Pd nanoparticles with uniform shape and size. *Journal of the American Chemical Society*, 127(20):7332-7333, 2005

[11] Iravani, S. Green synthesis of metal nanoparticles using plants. *Green Chemistry*, 13(10):2638-2650, 2011.

[12] Ankamwar, B., Damle, C., Ahmad, A., and Sastry, M. Biosynthesis of gold and silver nanoparticles using *Emblica officinalis* fruit extract, their phase transfer and transmetallation in an organic solution. *Journal of Nanoscience and Nanotechnology*, 5(10):1665-1671, 2005.

[13] Mittal, A. K.,Chisti, Y., and Banerjee, U. C. Synthesis of metallic nanoparticles using plant extracts. *Biotechnology advances*, 31(2) 346-356, 2013.

[14] Roopan, S. M., Bharathi, A., Kumar, R., Khanna, V. G., and Prabhakarn, A. Acaricidal, insecticidal, and larvicidal efficacy of aqueous extract of Annona squamosa L peel as biomaterial for the reduction of palladium salts into nanoparticles. *Colloids and Surfaces B: Biointerfaces*, 92:209-212, 2012.

[16] Sheny, D. S., Philip, D., and Mathew, J. Rapid green synthesis of palladium nanoparticles using the dried leaf of Anacardium occidentale. *Spectrochimica Acta Part A: Molecular and Biomolecular Spectroscopy*, 91:35-38, 2012.

[17] Sathishkumar, M., Sneha, K., Kwak, I. S., Mao, J.,Tripathy, S. J., and Yun, Y. S. Phyto-crystallization of palladium through reduction process using Cinnamom zeylanicum bark extract. *Journal of Hazardous materials*, 171(1-3):400-404, 2009.

[18] Bankar, A., Joshi, B., Kumar, A. R., and Zinjarde, S. Banana peel extract mediated novel route for the synthesis of palladium nanoparticles. *Materials Letters*, 64(18):1951-1953, 2010.

[19] Xu, L., Wu, X. C., and Zhu, J. J. Green preparation and catalytic application of Pd nanoparticles. *Nanotechnology*, 19(30):305603, 2008.

[20] Zhou, P., Wang, H., Yang, J., Tang, J., Sun, D., and Tang, W. Bacteria cellulose nanofibers supported palladium (0) nanocomposite and its catalysis evaluation in Heck reaction. *Industrial & Engineering Chemistry Research*, 51(16):5743-5748, 2012.

[21] Huang, A. S., Titchenal, C. A., and Meilleur, B. A. Nutrient composition of taro corms and breadfruit. *Journal of Food Composition and Analysis*, 13(5):859-864, 2000.

[22] Barua, S., Konwarh, R., Mandal, M., Gopalakrishnan, R., Kumar, D., and Karak, N. Biomimetically prepared antibacterial, free radical scavenging poly(ethyleneglycol) supported silver nanoparticles as Aedes albopictus larvicide. *Advanced Science, Engineering and Medicine*, 5(4):291-298, 2013.